

REPORT DOCUMENTATION PAGE

Form Approved
OMB No. 0704-0188

Public reporting burden for this collection of information is estimated to average 1 hour per response, including the time for reviewing instructions, searching existing data sources, gathering and maintaining the data needed, and completing and reviewing this collection of information. Send comments regarding this burden estimate or any other aspect of this collection of information, including suggestions for reducing this burden to Department of Defense, Washington Headquarters Services, Directorate for Information Operations and Reports (0704-0188), 1215 Jefferson Davis Highway, Suite 1204, Arlington, VA 22202-4302. Respondents should be aware that notwithstanding any other provision of law, no person shall be subject to any penalty for failing to comply with a collection of information if it does not display a currently valid OMB control number. PLEASE DO NOT RETURN YOUR FORM TO THE ABOVE ADDRESS.

1. REPORT DATE (DD-MM-YYYY) 04-01-2006	REPRINT	5a. CONTRACT NUMBER
4. TITLE AND SUBTITLE QUANTUM LATTICE GAS REPRESENTATION FOR VECTOR SOLITONS		5b. GRANT NUMBER
		5c. PROGRAM ELEMENT NUMBER 61102F
6. AUTHOR(S) G. Vahala*, L. Vahala**, and J. Yepez		5d. PROJECT NUMBER 2304
		5e. TASK NUMBER 0T
		5f. WORK UNIT NUMBER B1
7. PERFORMING ORGANIZATION NAME(S) AND ADDRESS(ES) Air Force Research Laboratory/VSBYA 29 Randolph Road Hanscom AFB MA 01731-3010		8. PERFORMING ORGANIZATION REPORT NUMBER AFRL-VS-HA-TR-2005-1203
9. SPONSORING / MONITORING AGENCY NAME(S) AND ADDRESS(ES)		10. SPONSOR/MONITOR'S ACRONYM(S)
		11. SPONSOR/MONITOR'S REPORT NUMBER(S)

12. DISTRIBUTION / AVAILABILITY STATEMENT

Approved for Public Release; Distribution Unlimited.

*Dept Physics, College of William & Mary, Williamsburg, VA

**Dept Electrical & Comp Engr, Old Dominion University, Norfolk, VA

13. SUPPLEMENTARY NOTES

REPRINTED FROM: Quantum Information and Computation, edited by E.J. Donkor, A.R. Pirich, H.E. Brandt, PROCEEDINGS OF SPIE, Vol 5105(SPIE, Bellingham, WA 2003)

14. ABSTRACT

Quantum lattice gas algorithms are developed for the coupled-nonlinear Schrodinger (coupled-NLS) equations, equations that describe the propagation of pulses in birefringent fibers. When the cross-phase modulation factor is unity, the coupled-NLS reduce to the Manakov equations. The quantum lattice gas algorithm yields vector solitons for the fully integrable Manakov system that are in excellent agreement with exact results. Simulations are also presented for the interaction between a turbulent 2-soliton mode and a simple NLS 2-soliton mode. The quantum algorithm requires 4 qubits for each spatial node, with quantum entanglement required only between pairs of qubits through a unitary collision operator. The coupling between the qubits is achieved through a local phase change in the absolute value of the paired qubit wave functions. On symmetrizing the unitary streaming operators, the resulting quantum algorithm, which is unconditionally stable, is accurate to $O(\epsilon^2)$.

15. SUBJECT TERM:

Vector solitons Coupled-NLS Manakov equations
Quantum lattice gas algorithms Turbulence

16. SECURITY CLASSIFICATION OF:		17. LIMITATION OF ABSTRACT SAR	18. NUMBER OF PAGES	19a. NAME OF RESPONSIBLE PERSON Jeffrey Yepez
a. REPORT UNCLAS	c. THIS PAGE UNCLAS			19b. TELEPHONE NUMBER (include area code) 781-377-5957

Quantum Lattice Gas Representation for Vector Solitons

George Vahala^a, Linda Vahala^b, Jeffrey Yepez^c

^aDept. of Physics, William & Mary, Williamsburg, VA 23187

^bDept. of Electrical & Computer Engineering, Old Dominion University, Norfolk, VA 23529

^cAir Force Research Laboratory, Hanscom AFB, MA 01731

ABSTRACT

Quantum lattice gas algorithms are developed for the coupled-nonlinear Schrodinger (coupled-NLS) equations, equations that describe the propagation of pulses in birefringent fibers. When the cross-phase modulation factor is unity, the coupled-NLS reduce to the Manakov equations. The quantum lattice gas algorithm yields vector solitons for the fully integrable Manakov system that are in excellent agreement with exact results. Simulations are also presented for the interaction between a turbulent 2-soliton mode and a simple NLS 2-soliton mode. The quantum algorithm requires 4 qubits for each spatial node, with quantum entanglement required only between pairs of qubits through a unitary collision operator. The coupling between the qubits is achieved through a local phase change in the absolute value of the paired qubit wave functions. On symmetrizing the unitary streaming operators, the resulting quantum algorithm, which is unconditionally stable, is accurate to $O(\epsilon^2)$.

Keywords : vector solitons, coupled-NLS, Manakov equations, quantum lattice gas algorithms, turbulence

1. INTRODUCTION

One of the most fundamental equations of soliton physics is the nonlinear Schrodinger equation (NLS)

$$i \frac{\partial \psi}{\partial t} + \frac{\partial \psi}{\partial x^2} + V[\psi] \psi = 0 \quad (1)$$

which can describe the propagation of optical solitons in an ideal fiber. However, in reality, optical fibers are birefringent and a single mode fiber can support two distinct orthogonal polarizations. One of these modes is the O-mode and has constant refractive index along the ray path while the other mode is the X-mode whose refractive index varies along the ray path. Thus the pulses will travel down with slightly different speeds along the two orthogonal polarization axes. Proceeding from the electromagnetic wave equation for the electric field \mathbf{E} in a dielectric medium

$$\nabla^2 \mathbf{E} - \frac{1}{c^2} \frac{\partial^2 \mathbf{E}}{\partial t^2} = -\mu_0 \frac{\partial^2 \mathbf{P}}{\partial t^2} \quad (2)$$

where the polarization \mathbf{P} represents the linear and nonlinear induced polarization, it can be shown [1] that the slowly varying amplitudes of these modes satisfy the coupled-NLS equations

$$i \frac{\partial Q_1}{\partial t} + \frac{\partial^2 Q_1}{\partial x^2} + 2\mu [|Q_1|^2 + B |Q_2|^2].Q_1 = 0, \quad i \frac{\partial Q_2}{\partial t} + \frac{\partial^2 Q_2}{\partial x^2} + 2\mu [|Q_2|^2 + B |Q_1|^2].Q_2 = 0 \quad (3)$$

Here μ is a positive parameter and B is the cross-phase modulational coefficient, $B = (2 + 2\sin^2 \theta) / (2 + \cos^2 \theta)$, where $0 \leq \theta \leq \pi/2$ is the birefringence ellipticity angle [2]. The coupled-NLS equations (3) are generally nonintegrable, except for the special case of $B=1$ in which they reduced to the completely integrable Manakov equations [3]. The Manakov equations are completely integrable, with soliton solutions. For a linearly birefringent fiber $B=2/3$. The coupled-NLS equations also arise in spatial beam propagation in crystals [4], and under special circumstances $B=1$, yielding the soliton Manakov system.. These Manakov equations also describe propagation in randomly birefringent fibers [5].

Here we develop a quantum lattice gas representation of the more general coupled-NLS equations for linear coupling potentials V_1 and V_2 :

20060117 473

$$i \frac{\partial Q_1}{\partial t} + \frac{\partial^2 Q_1}{\partial x^2} + V_1[|Q_1|, |Q_2|] \cdot Q_1 = 0 \quad , \quad i \frac{\partial Q_2}{\partial t} + \frac{\partial^2 Q_2}{\partial x^2} + V_2[|Q_2|, |Q_1|] \cdot Q_2 = 0 \quad (4)$$

which is unconditionally stable and ideal for implementation (and parallelization) on a hybrid quantum-classical computer [6] as well as on a classical computer. This representation is a generalization of our earlier work [7] on quantum algorithms for the simple NLS and KdV solitons, which was based on the quantum algorithm for the (linear) Schrodinger equation [8]. These quantum lattice gas algorithms can, in principle, be modeled on a liquid NMR quantum computer [9-13]. The exponential speed-up over classical computers arises from the quantum entanglement of qubits. In Sec. 2 we briefly summarize the quantum lattice gas algorithm for 4 qubits/lattice. The unitary collision and streaming operators entangle just pairs of qubits. The local coupling of all the qubits is achieved by introduce a phase change into the wave functions. This phase change (for each qubit pair) allows for the introduction of an "external" potential and the modeling of vector soliton physics. For the liquid NMR computer, one needs only hold the phase coherence for 16 gate operations before measurements are needed in order to determine the potentials. Vector soliton collisions are then studied with this algorithm in Sec. 3, for both the Manakov system as well as for the nonintegrable case of $B \neq 1$ and for vector soliton turbulence. Excellent agreement is found for both the vector 1-soliton and 2-soliton solutions of the Manakov system.

2. QUANTUM LATTICE GAS REPRESENTATION FOR COUPLED-NLS

We first discretize the spatial domain into L lattice nodes so that the wave function ψ has a basis ket $|x_1\rangle$ -expansion

$$|\psi\rangle = \sum_{l=1}^L c_l |x_l\rangle \quad , \text{ with } c_l = \langle x_l | \psi \rangle \quad (5)$$

being the probability amplitude associated with the ket $|x_l\rangle$. For the coupled-NLS equations we introduce 4 qubits at each lattice node $l : |q_a^1\rangle$, $a = 0, 1, 2, 3$. Each qubit is a two-level quantum system

$$|q_a^1\rangle = \alpha_a^1 |0\rangle + \beta_a^1 |1\rangle \quad , \text{ with } |\alpha_a^1|^2 + |\beta_a^1|^2 = 1 \quad , \quad a = 0 \dots 3 \quad ; \quad l = 1 \dots L \quad (6)$$

In the number representation one can employ binary indexing for the basis set

$$|n_0^1 n_1^1 n_2^1 n_3^1 \dots n_0^L n_1^L n_2^L n_3^L\rangle \quad \text{where } n_{0,1}^1 = 0 \text{ or } 1 \quad , \quad \forall l \text{ and } n_{2,3}^1 = 0 \text{ or } 1 \quad , \quad \forall l \quad (7)$$

which factors since only the qubits $|q_{0,1}^1\rangle$ will be entangled with each other and similarly for the entanglement of the qubits $|q_{2,3}^1\rangle$ at each spatial site:

$$|n_0^1 n_1^1 \dots n_0^L n_1^L\rangle |n_2^1 n_3^1 \dots n_2^L n_3^L\rangle \quad (8)$$

We can restrict ourselves to the one-particle sectors for qubits $|q_{0,1}^1\rangle$ and qubits $|q_{2,3}^1\rangle$ in which the basis set elements in Eq. (8) have only one $n_{0,1}^1$ that is 1 while all the other $n_{0,1}^1$ are zero, and similarly for $n_{2,3}^1$. In essence, for the two qubits $|q_{0,1}^1\rangle$, there are $2L$ such elements which can be labeled using the binary scheme $|2^{21+a}\rangle$, $l = 1 \dots L$, $a = 0, 1$ so that in this binary scheme the wave function corresponding to the two qubits $|q_{0,1}^1\rangle$

$$|\psi\rangle_{01} = \sum_{l=1}^L \sum_{a=0}^1 \xi_{2l+a} |2^{21+a}\rangle \quad . \quad (8)$$

Interference effects between the two qubits $|q_{0,1}^1\rangle$ at each position ket $|x_l\rangle$ can be achieved by setting

$$c_1 = \xi_{2l-1} + \xi_{2l} \quad (9)$$

Similarly for the interference effects between the two qubits $|q_{2,3}^1\rangle$. To recover the coupled-NLS equations we do not need to enforce interference effects between all four qubits at the spatial node $|x_l\rangle$. Hence, for simplicity, we now just concentrate on the application of the unitary collision and streaming operator to the two qubits $|q_{0,1}^1\rangle$ -- exactly the same unitary and streaming operators will be applied to the two qubits $|q_{2,3}^1\rangle$.

2.1 Unitary collision operator for the qubit-pair $|q_{0,1}\rangle$

To evolve the wave function for the two qubits $|q_{0,1}\rangle$ in time, a quantum unitary operator \widehat{C} is constructed from a tensor product of quantum gates, each independently applied on a site-to-site basis

$$\widehat{C} = \bigotimes_{l=1}^L \widehat{U}_1 \quad (10)$$

Quantum entanglement arises from the on-site local unitary collision operator \widehat{U}_1 acting on the 2 qubits $|q_{0,1}\rangle$ at each node; i.e., \widehat{U}_1 acts on the 4 on-site basis kets for $|q_{0,1}\rangle$:

$$|0\rangle \otimes |0\rangle = |1000\rangle, |0\rangle \otimes |1\rangle = |0100\rangle, |1\rangle \otimes |0\rangle = |0010\rangle, |1\rangle \otimes |1\rangle = |0001\rangle$$

In particular, \widehat{U}_1 acts on the on-site ket $|v\rangle = |0\rangle \otimes |1\rangle + |1\rangle \otimes |0\rangle = |0110\rangle$. A local equilibrium can be associated with this on-site unitary collision operator if $|v\rangle$ is an eigenvector of \widehat{U}_1 with unit eigenvalue : $\widehat{U}_1|v\rangle = |v\rangle$.

To recover NLS, we introduce the square-root-of-swap gate $\widehat{U}_1 = \widehat{U}$ on a site-by-site basis [8]

$$\widehat{U}_{NLS} = \begin{pmatrix} 1 & 0 & 0 & 0 \\ 0 & \frac{1-i}{2} & \frac{1+i}{2} & 0 \\ 0 & \frac{1+i}{2} & \frac{1-i}{2} & 0 \\ 0 & 0 & 0 & 1 \end{pmatrix} \quad (11)$$

In the number representation \widehat{U}_{NLS} acts on the kets $|2^{21-1}\rangle$ and $|2^{21}\rangle$ for the two qubits $|q_{0,1}\rangle$ on the site $\{x_1\}$.

Moreover, a Hamiltonian representation for this unitary quantum gate \widehat{U}_{NLS} can be achieved from appropriate tensor products of the Pauli spin matrices $\sigma_x = \begin{pmatrix} 0 & 1 \\ 1 & 0 \end{pmatrix}$, $\sigma_y = \begin{pmatrix} 0 & -i \\ i & 0 \end{pmatrix}$, and $\sigma_z = \begin{pmatrix} 1 & 0 \\ 0 & -1 \end{pmatrix}$ for qubits '0' and '1' :

$$\widehat{U}_{NLS} = \exp\left[\frac{i\pi}{8}\right] \exp\left[-\frac{i\pi}{8}(\sigma_x^1 \sigma_x^2 + \sigma_y^1 \sigma_y^2 + \sigma_z^1 \sigma_z^2)\right] \quad (12)$$

with $\widehat{U}_{NLS}^4 = I$, the identity operator so that $\widehat{U}_{NLS}^4 |v\rangle = |v\rangle$.

2.2 Unitary Streaming Operator for the qubit-pair $|q_{0,1}\rangle$

The next step of the quantum lattice gas algorithm is to stream the post-collision on-site ket for qubits $|q_{0,1}\rangle$ to nearest neighbor sites. The (unitary) streaming operator \widehat{S}_1 is defined as a global shift to the right of only qubit $|q_0\rangle$ on each lattice node, i.e.,

$$\widehat{S}_1 = \prod_{l=1}^{L-1} \widehat{\chi}_{21-l, 21+l} \quad (13)$$

where $\widehat{\chi}_{21-l, 21+l}$ is independent of l and in the number representation shifts the amplitude of the ket $|2^{21-1}\rangle$ on site $\{x_1\}$ to the ket $|2^{21+l}\rangle$ on site $\{x_{l+1}\}$ for the qubit-pair $|q_{0,1}\rangle$. In matrix form, the qubit streaming operator $\widehat{\chi}$ is a $2^2 \times 2^2$ (unitary) permutation matrix

$$\widehat{\chi} = \begin{pmatrix} 1 & 0 & 0 & 0 \\ 0 & 0 & 1 & 0 \\ 0 & 1 & 0 & 0 \\ 0 & 0 & 0 & 1 \end{pmatrix} \quad (14)$$

Thus, for the two-qubit pair $|q_{0,1}\rangle$, \widehat{U} operates on the on-site qubits while $\widehat{\chi}$ operates on the 1st qubit of neighboring sites. Hence the total collision matrix \widehat{C} does not commute with the streaming operator \widehat{S}_1 . To symmetrize the

algorithm, we also introduce the streaming operator \hat{S}_2 that performs a global shift to the right of the 2nd qubit on all the lattice nodes for the qubit-pair $|q_{0,1}\rangle$:

$$\hat{S}_2 = \prod_{l=1}^{L-1} \hat{\chi}_{2l,2l+2} \quad (15)$$

2.3 Introduction of the Potential Field for the qubit-pair $|q_{0,1}\rangle$

It has been shown [14, 8] that the effect of an external potential $V_1(x)$ can be modeled by the introduction of a local phase change to the system wave function for the qubit-pair $|q_{0,1}\rangle$. Let Q_1 denote the wave function for the qubit-pair $|q_{0,1}\rangle$, and Q_2 for the qubit pair $|q_{2,3}\rangle$. Thus

$$Q_1(x,t) \rightarrow \exp[iV_1(x)\Delta t] Q_1(x,t) \quad (16)$$

where Δt is the time advancement after each step of the algorithm.

Similarly, for the qubit-pair $|q_{2,3}\rangle$. One can introduce another external potential $V_2(x)$ by a local phase change in the system wave function Q_2 for the qubit-pair $|q_{2,3}\rangle$:

$$Q_2(x,t) \rightarrow \exp[iV_2(x)\Delta t] Q_2(x,t) \quad (17)$$

2.4 Quantum algorithm for coupled-NLS

We simultaneously apply the collide-stream sequence of unitary operators to the qubit pairs $|q_{0,1}\rangle$ and $|q_{2,3}\rangle$

$$\begin{pmatrix} Q_1(t+\Delta t) \\ Q_2(t+\Delta t) \end{pmatrix} = \begin{pmatrix} [\hat{S}_2^T \hat{C} \hat{S}_2 \hat{C} \hat{S}_2^T \hat{C} \hat{S}_2 \hat{C} \hat{S}_1^T \hat{C} \hat{S}_1 \hat{C} \hat{S}_1^T \hat{C} \hat{S}_1 \hat{C}] Q_1(t) \\ [\hat{S}_2^T \hat{C} \hat{S}_2 \hat{C} \hat{S}_2^T \hat{C} \hat{S}_2 \hat{C} \hat{S}_1^T \hat{C} \hat{S}_1 \hat{C} \hat{S}_1^T \hat{C} \hat{S}_1 \hat{C}] Q_2(t) \end{pmatrix} \quad (18)$$

where \hat{S}_i^T is the transpose of \hat{S}_i , with $\hat{S}_i^T \hat{S}_i = I$, $i=1,2$ and \hat{C} is based on the unitary collision operator \hat{U}_{NLS} , Eq. (11). We then apply the phase change transformations (16), (17) following the collide-stream sequence :

$$\begin{pmatrix} Q_1 \\ Q_2 \end{pmatrix} \rightarrow \begin{pmatrix} \exp[V_1(|Q_1|,|Q_2|)\Delta t] \cdot Q_1 \\ \exp[V_2(|Q_1|,|Q_2|)\Delta t] \cdot Q_2 \end{pmatrix} \quad (19)$$

where the potential fields are required to be functions of the wave functions themselves $V_i = V_i(|Q_1|,|Q_2|)$

The continuum limit is defined by scaling the spatial shift between neighboring nodes to be $O(\epsilon)$, the time advancement $\Delta t = O(\epsilon^2)$ and the potentials $V_i = \epsilon^2 V_i(|Q_1|,|Q_2|)$. In the limit $\epsilon \rightarrow 0$, it can be shown using Mathematica that the Eq. (18)-(19) sequence yields the coupled-NLS equations

$$\begin{aligned} i \frac{\partial Q_1}{\partial t} + \frac{\partial^2 Q_1}{\partial x^2} + V_1(|Q_1|,|Q_2|) \cdot Q_1 &= 0 + O(\epsilon^2), \\ i \frac{\partial Q_2}{\partial t} + \frac{\partial^2 Q_2}{\partial x^2} + V_2(|Q_1|,|Q_2|) \cdot Q_2 &= 0 + O(\epsilon^2) \quad , \quad \text{as } \epsilon \rightarrow 0 \end{aligned} \quad (20)$$

with error of $O(\epsilon^2)$. Equation (20) holds for any choice of potentials V_1 and V_2 .

It is now clear how to extend this analysis to a system of N-coupled NLS equations. N-coupled NLS equations arise in the study of beam propagation in a Kerr-like photorefractive medium, which typically exhibits very strong nonlinear effects with extremely low optical powers. Partially coherent solitons have been observed through excitation by partially coherent light [15] as well as by ordinary incandescent light bulb [16].

3. QUANTUM LATTICE GAS SIMULATIONS FOR COUPLED-NLS

3.1 Vector soliton Manakov system

We first test our quantum algorithm on the fully integrable Manakov system

$$i \frac{\partial Q_1}{\partial t} + \frac{\partial^2 Q_1}{\partial x^2} + 2\mu [|Q_1|^2 + |Q_2|^2] \cdot Q_1 = 0, \quad i \frac{\partial Q_2}{\partial t} + \frac{\partial^2 Q_2}{\partial x^2} + 2\mu [|Q_2|^2 + |Q_1|^2] \cdot Q_2 = 0 \quad (21)$$

with the cross-phase modulation coefficient $B = 1$. The 1-soliton vector solution is [17]

$$Q_1(x, t) = \frac{\alpha}{2} \exp \left[-\frac{R}{2} + i\eta_I \right] \operatorname{Sech} \left[\eta_R + \frac{R}{2} \right], \quad Q_2(x, t) = \frac{\beta}{\alpha} Q_1(x, t) \quad (22)$$

where $\eta = k(x + i k t)$ and α, β, k are arbitrary complex parameters with subscripts R and I denoting the real and imaginary parts. $R = \ln [\mu (|\alpha|^2 + |\beta|^2) / (k + k^*)^2]$ is real and $k_R \neq 0$.

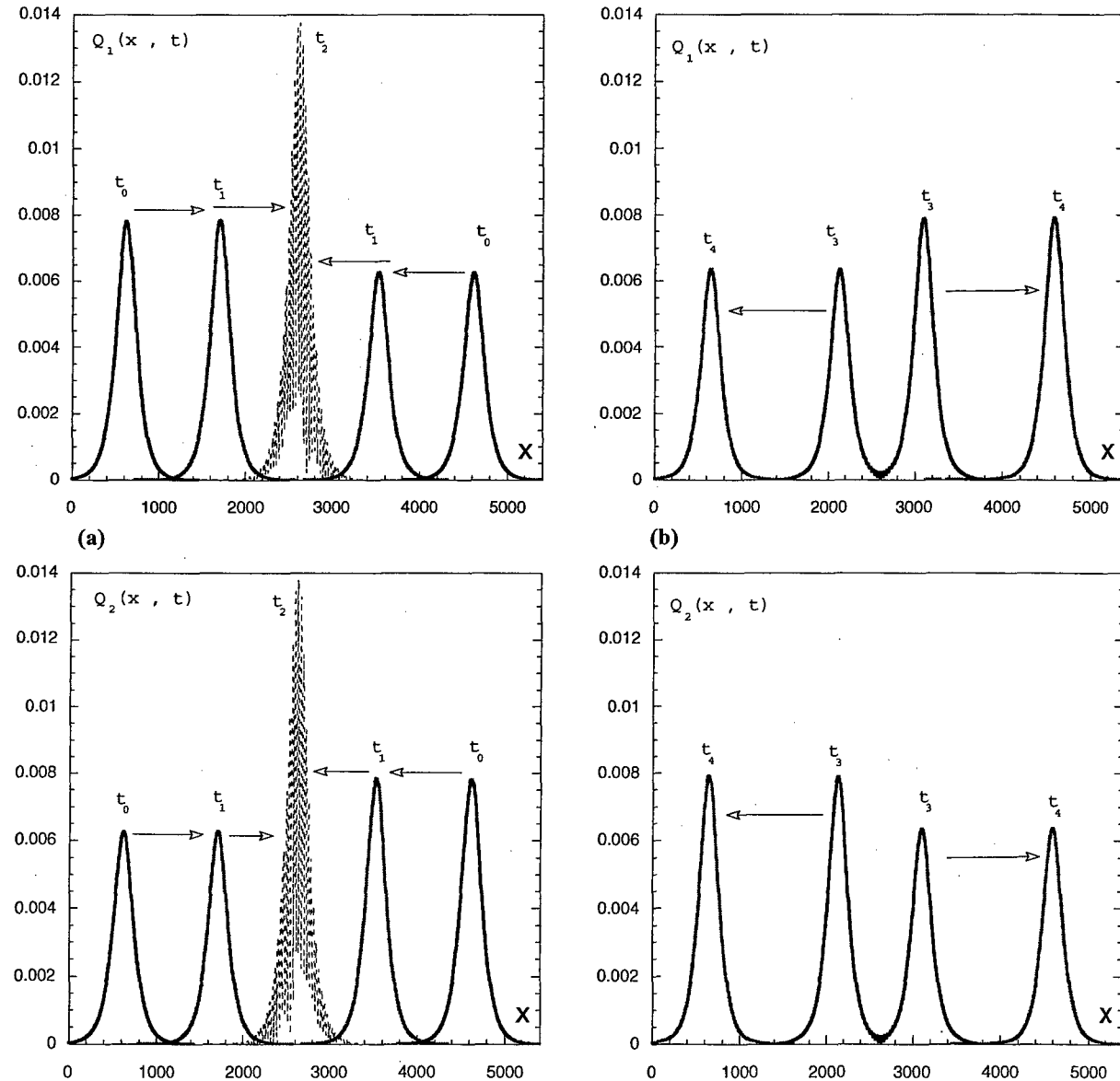


Fig. 1 The Vector 2-soliton Manakov solution [$B = 1$] for (a) pre-collision and (b) post-collision times for the two orthogonal polarization direction $Q_1(x, t)$ and $Q_2(x, t)$. Initially ($t = t_0$), the 2-solitons of the Q_1 -mode are at $x = 615$ and $x = 4605$ with the larger amplitude soliton moving \rightarrow while the lower amplitude soliton has the same speed but moving \leftarrow . For the 2-solitons of the Q_2 -mode, the smaller amplitude soliton at $x = 615$ moves in \rightarrow while the larger amplitude soliton at $x = 4605$ moves in \leftarrow . The 2-vector soliton collision is elastic as seen at the snapshots: $t_0 = 0$, $t_1 = 5.5$ K, $t_2 = 10$ K (collision - strong wave function overlaps), $t_3 = 12.5$ K and $t_4 = 20$ K iterations.

For non-overlapping solitons, the initial (t_0) 2-soliton states for the Q_1 - and Q_2 -modes reduce to the simple 1-soliton wave functions of the form given by Eq. (22). The vector elastic collision of these 2-soliton modes is clear.

3.2 Integrable-Nonintegrable Coupled-NLS

We now consider the following evolution equations for the Q_1 - and Q_2 -modes:

$$i \frac{\partial Q_1}{\partial t} + \frac{\partial^2 Q_1}{\partial x^2} + 2\mu [|Q_1|^2 + |Q_2|^2] \cdot Q_1 = 0, \quad i \frac{\partial Q_2}{\partial t} + \frac{\partial^2 Q_2}{\partial x^2} + \sqrt{2\mu [|Q_2|^2 + |Q_1|^2]} \cdot Q_2 = 0 \quad (23)$$

with the same initial conditions as in the Manakov system:

$$Q_1(x, t) = \frac{\alpha}{2} \exp \left[-\frac{R}{2} + i\eta_I \right] \text{Sech} \left[\eta_R + \frac{R}{2} \right], \quad Q_2(x, t) = \frac{\beta}{\alpha} Q_1(x, t) \quad (24)$$

In our earlier work [7], for the scalar nonintegrable NLS for the uncoupled Q_2 -mode, the Q_2 -mode exhibited soliton turbulence [18]. Here we shall see that the coupling of these two modes will drive the Q_1 -mode out of its quasi-soliton state because of its coupling to the turbulent Q_2 -mode.

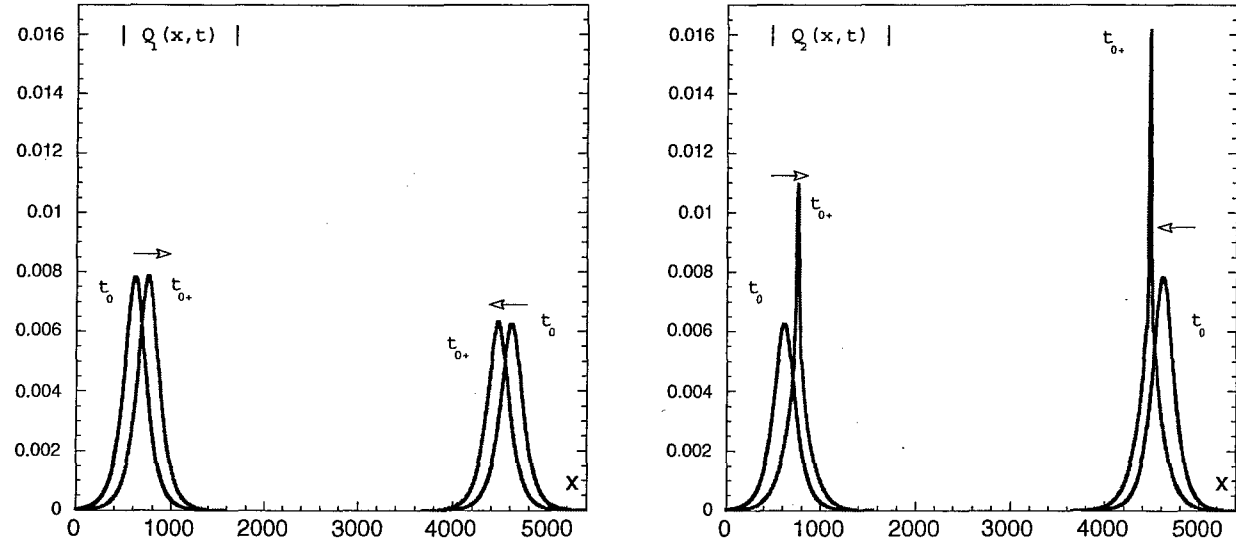


Fig. 2 The initial pulses for the Q_1 - and Q_2 -modes ($t_0 = 0$) which are the 2-soliton vector solutions for the Manakov system, Fig. 1. At $t_{0+} = 0.7$ K, the Q_1 -mode retains the vector 2-soliton structure while the Q_2 -wave function undergoes very significant contraction, although the group velocities of these pulses are unaffected by the nonintegrable coupling potentials and remain equal to the Manakov group velocities.

The quasi-integrable Q_1 -mode, in the early time evolution, retains its Manakov-like soliton solution (Fig. 2) for early times ($t_{0+} = 0.7$ K) because of the weak coupling to the nonintegrable Q_2 -mode which rapidly loose their Manakov-like structure and become more localized structures. However, the structures retain their Manakov-like group velocities.

While the nonintegrable Q_2 -mode retains its sharp structures (Fig. 3 with $t_1 = 1.4 K$), but small amplitude sidebands form and then start to rapidly move away from the sharp structure ($t_2 = 5.5 K$). The coupling of the Q_1 - and Q_2 -modes now distorts the quasi-Manakov Q_1 -solitons with slight contraction and higher peak together with the emission of very weak sidebands (Fig. 3).

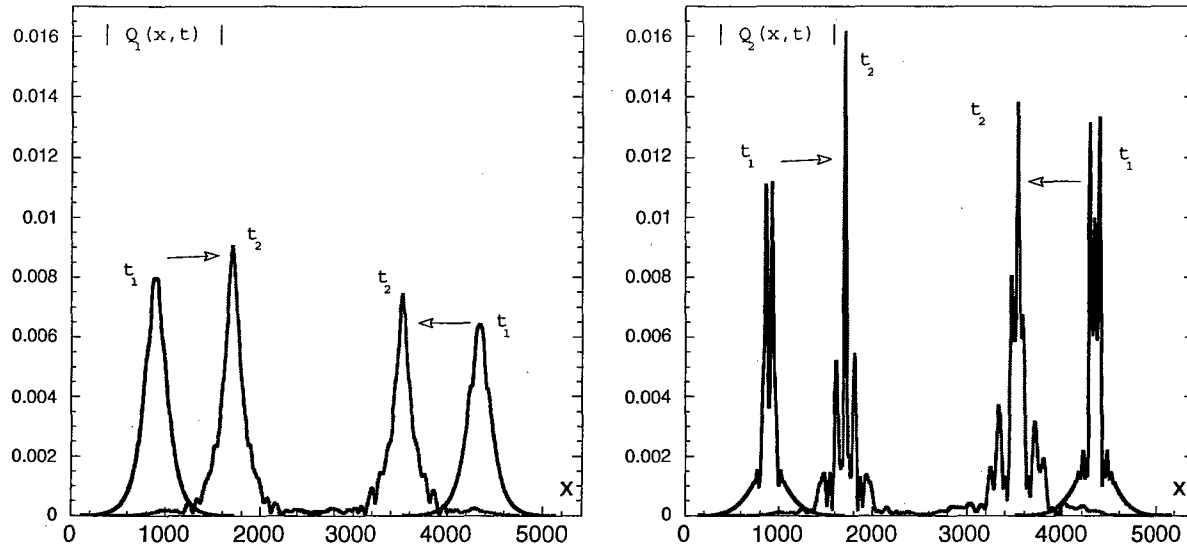


Fig. 3 The evolution of $|Q_1|, |Q_2|$ at times $t_1 = 1.4 K$ and $t_2 = 5.5 K$. The quasi-Manakov Q_1 -solitons are slightly compressed due to the coupling with the nonintegrable Q_2 -structures which become very sharp and emit weak sidebands.

As these mode develop in time, Fig. 4, one notes that the all the structures in the Q_2 -mode, both the very sharp large amplitude peaks and the broadband 'noise' with rapidly moving weaker fine structures, behave like quasi-solitons : i.e.,

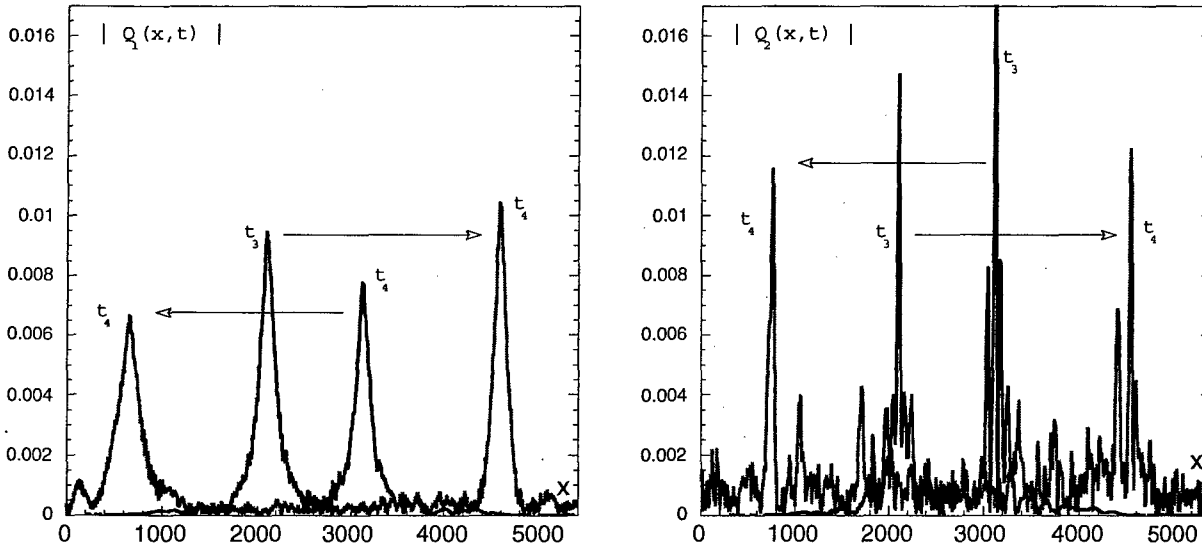


Fig. 4 The Q_1 - and Q_2 -modes at times $t_3 = 7.5 K$ and $t_4 = 20 K$. The sharp structures in the Q_2 -mode behave like quasi-solitons in their interaction : the rapidly moving sharp small amplitude structures (with varying group velocities in both directions) pass through each other as well as through the slowly moving large scale structures.

these fine-scale structures are transparent not only to other fine-scale structures, but also transparent to the slowly moving sharp large-scale structures. In essence, one can refer to this as soliton turbulence. The coupling to the Q_1 -mode leads to the Q_1 quasi-solitons being broadened further with the emission of broadband 'noise'. The Q_2 -large scale structure maxima rapidly pulsates in a way very reminiscent of the periodic pulsating bound 2-soliton solution for the simple NLS [19].

In Fig. 5 we plot the Q_1 - and Q_2 -modes at $t = 50$ K and $t = 110$ K to contrast their different time evolution. It is apparent that the group velocity of the large scale structures in both modes are unchanged by the coupling. Both modes exhibit soliton turbulence while the Q_1 -mode's major 2 structures still retain their identity, albeit broadened. The initial Q_2 -mode's major 2 structures (see Fig. 2) have been destroyed, as can be seen in Fig. 5 at $t = 110$ K.

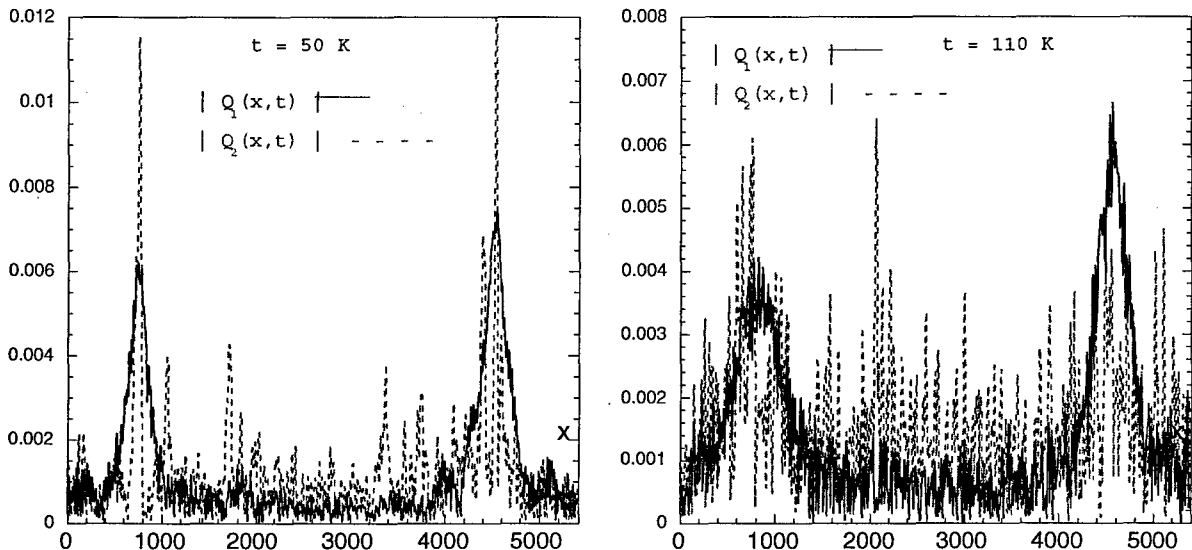


Fig. 5 The Q_1 - and Q_2 -modes at $t = 50$ K and $t = 110$ K. The major peaks in the Q_2 -mode pulsate not unlike the 2-soliton bound solution for simple NLS, except that for the Q_2 -mode the major peaks have a non-zero drift velocity. The lower amplitude peaks that are superimposed on the broadband noise act like soliton turbulence.

4. CONCLUSION

A quantum lattice gas representation is developed for the solution of coupled-NLS equations, equations that can model the propagation of pulses down a birefringent fiber. The quantum algorithm requires 4 qubits per spatial node, with the unitary collision and streaming operators coupling qubit pairs. The qubit pairs are then coupled to each other by the introduction of appropriate phase changing potentials to the qubit pair wave functions. Quantum phase coherence needs to be enforced for only 16 quantum gate operations since measurements need then be taken to determine the absolute value of the wave functions so as to be able to initialize the quantum computer for the next time evolution stage. It is interesting to note that a liquid NMR quantum computer [13] has recently been used to accurately solve the diffusion equation using a quantum lattice gas algorithm. Since the quantum mechanical sites communicate with each other classically, this architecture has been dubbed a Type-II quantum computer [6]. The Type-II quantum computer networks many small quantum processors. Given this preliminary experimental success, it appears at least possible that the quantum algorithm presented here may be run on an actual Type-II quantum computer in the future. However, the quantum algorithm for vector solitons would be very difficult to implement experimentally. Even though a one-dimensional model, it is sufficiently complex because amplitudes must be extracted from the quantum measurement process and not simply probabilities which are more naturally extracted from the projective von Neumann quantum measurement process over a large ensemble of molecules as occurs in NMR spectroscopy. The fact that amplitudes, instead of binary bits or probabilities, must be extracted from the quantum measurement is what makes the experimental

implementation much less efficient than otherwise. Nevertheless, it is hoped that this one-dimensional quantum algorithm serves as a stepping stone towards more complicated quantum algorithms with sufficiently many qubits per site so that the experimental trade-off between the difficulty of achieving quantum entanglement and the severe limitation of measurable classical information that can be extracted from the quantum computer begins to work in our favor. Finally, it is interesting to note that the quantum lattice gas representation is very efficiently parallelized on a classical computer.

ACKNOWLEDGMENTS

This work was supported by the Directorate of Computational Mathematics, Air Force Office of Scientific Research.

REFERENCES

- [1] M. Lakshmanan and T. Kanna, *Pramana - J. Phys.* **57**, 885 (2001)
- [2] C. R. Menyuk, *IEEE J. Quantum Electron.* **QE-25**, 2674 (1989)
- [3] S. V. Manakov, *Sov. Phys. JETP* **38**, 248 (1974).
- [4] J. U. Kang, G. I. Stegeman, J.S. Aitchison and N. Akhmediev, *Phys. Rev. Lett.* **76**, 3699 (1996)
- [5] T. I. Lakoba and D. J. Kaup, *Phys. Rev. E* **56**, 6147 (1997).
- [6] J. Yepez, *Intl. J. Modern Phys. C* **12**, 1273 (2001)
- [7] G. Vahala, J. Yepez and L. Vahala, *Phys. Lett. A* (to be published, 2003)
- [8] J. Yepez and B. M. Boghosian, *Comp. Phys. Comm.*, **146**, 280 (2002)
- [9] D. Bouwmeester, A. Ekert & A. Zeilinger (eds.) "The Physics of Quantum Information", Springer-Verlag, New York, 2000.
- [10] H-K. Lo, S. Popescu & T. Spiller (eds.) "Introduction to Quantum Computation and Information", World Scientific, Singapore, 1998.
- [11] M. A. Nielsen and I. L. Chuang, "Quantum Computation and Quantum Information", Cambridge Univ. Press, 2000.
- [12] M. Pravia, Z. Chen, J. Yepez and D. G. Cory, *Computer Phys. Comm* **146**, 339 (2002)
- [13] M. Pravia, Z. Chen, J. Yepez and D. G. Cory, *Phys. Rev. A*, to appear 2003
- [14] I. Bialynicki-Birula, *Phys. Rev. D* **49**, 6920 (1994)
- [15] M. Mitchell, Z. Chen, M. F. Shih and M. Segev, *Phys. Rev. Lett.* **77**, 490 (1997)
- [16] M. Mitchell and M. Segev, *Nature* **387**, 880 (1997).
- [17] R. Radhakrishnan, M. Lakshmanan and J. Hietarinta, *Phys. Rev. E* **56**, 2213 (1997)
- [18] R. Jordan and C. Josserand, *Phys. Rev. E* **61**, 1527 (2000).
- [19] M. Remoissenet, "Waves called Solitons", Springer-Verlag, New York (1994), p. 225